PHT APERTURES AND ABSOLUTE PHOTOMETRY

T. G. Müller, ISO Data Centre, ESA, Villafranca del Castillo, Spain

SAI/2000-051/Rp, Version 1.0, 9-Oct-2000

Abstract

Results from relative and absolute aperture photometry in 3 PHT-P filters (12, 25 and 60 μm) are presented. Relative signal sequences with the same filter and different apertures show the same trends for the FCS and for sky background measurements. It can therefore be concluded that the illumination from the FCS is flat. Comparison of absolute sky photometry with COBE/DIRBE measurements indicate that the apparent solid angles of PHT are off by 10 to 50%, depending on the filter and, for P2 25 μm, also on the brightness level. Measurement of f_{psf} values are consistent with theoretical values for the aperture range from 23″to 180″. With the combination of all results of this analysis it will be possible to understand and estimate the influences of **actual/default responses**, **point-/extended-/background sources** and **default/non-default apertures** in PHT-P measurements.

1 Introduction

The PHT-P photometric calibration was established with "default" apertures (see Table 5) and with point-sources (stars, asteroids and planets). But many observational programmes were performed with other apertures and the scientific targets are not always point-like. How do different apertures change the calibration? Do point- and extended sources show the same trends?

Aperture sequences on bright background positions show that the linearized signals do not scale with the aperture area (Müller 2000a). The same deviations can be found for FCS signals in different apertures. Point sources on the other hand are consistent with the theoretical point-spread function (Müller 2000b) for medium to large apertures. The absolute calibration of sky background measurements connects these two aspects: The FCS calibration, based on point-like celestial standards, has to be "transported" to extended sources via the solid angles of the apertures. Do the physical aperture sizes correspond to the apparent solid angles on the sky? How does a comparison with COBE-DIRBE look like?

Since the calibration measurements do not cover the full *filter-aperture-flux* parameter space, some exemplary measurements have been analysed. Only 3 filters have been considered: P1 12 μm, P2 25 μm and P3 60 μm. Only **staring** mode observations have been included.

In Sections 2 and 4 only normalized SCP signals have been used, without considering the absolute signal level. The signals have been divided by the corresponding aperture area (see Table 4) and then normalized to the default apertures (see Figures 1, 2 and 3). In Figures 7, 8 and 9 the normalization has been done in the 180″ aperture.

The Sections 3 and 5 include calibrated absolute fluxes for comparison with COBE-DIRBE values (in [MJy/sr]) and stellar models (in [Jy]). Here, the actual response of the detector (as determined by the FCS measurement) has been used to calculate the surface brightness (Section 3) or flux density (Section 5). Each section contains a description of the results and a short discussion. In the end the conclusions are given (Section 6).

2 Relative Aperture Sequences on Sky Background and FCS

Different multi-aperture sequences on the sky background and on the internal calibration source FCS have been analysed. The data reduction up to the SCP level is summarized in Appendix C. Signals have then been divided by the aperture area and normalized to the default apertures (see Table 5).

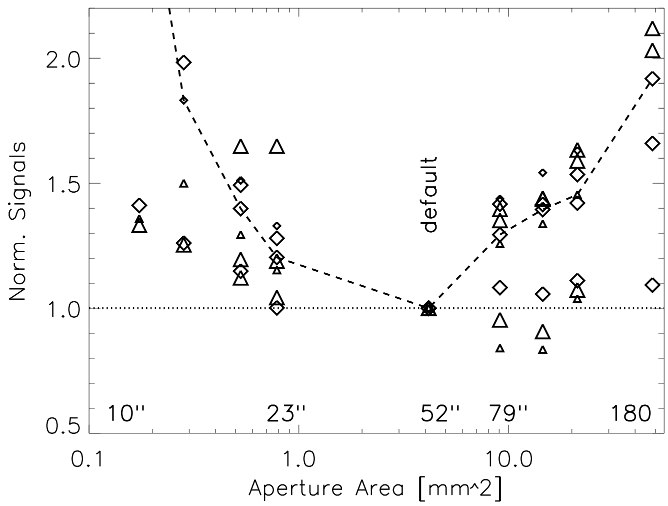

Aperture	Median	(Mean)
13″	1.83	(2.16)
18″	1.40	(1.58)
23″	1.20	(1.37)
52″	1.00	(1.00)
79″	1.29	(1.23)
99″	1.39	(1.26)
120″	1.45	(1.39)
180″	1.92	(1.76)

Figure 1: *P1, 12 μm: Measured sky signals (diamonds) and FCS signals (triangles), divided by aperture area and normalized to default aperture. The median (plotted) and mean deviations are given in the table.*

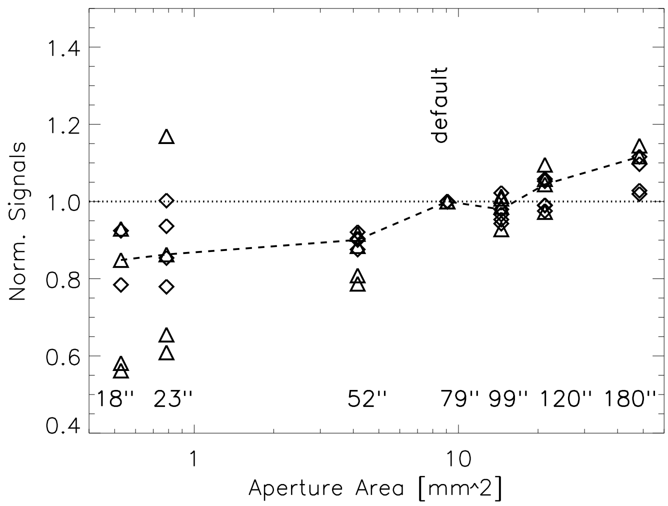

Aperture	Median	(Mean)
18″	0.84	(0.77)
23″	0.86	(0.86)
52″	0.90	(0.87)
79″	1.00	(1.00)
99″	0.98	(0.98)
120″	1.04	(1.03)
180″	1.12	(1.09)

Figure 2: *P2, 25 μm: Measured sky signals (diamonds) and FCS signals (triangles), divided by aperture area and normalized to default aperture. The median (plotted) and mean deviations are given in the table.*

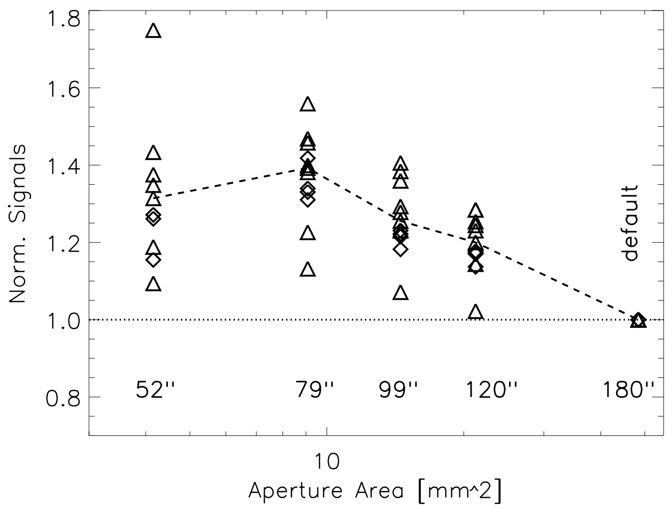

Aperture	Median	(Mean)
52″	1.31	(1.32)
79″	1.39	(1.37)
99″	1.26	(1.26)
120″	1.20	(1.19)
180″	1.00	(1.00)

Figure 3: *P3, 60 μm: Measured sky signals (diamonds) and FCS signals (triangles), divided by aperture area and normalized to default aperture. The median (plotted) and mean deviations are given in the table.*

2.1 Results

The 3 filters show a completely different behaviour: At 12 μm all apertures see more flux than expected (relative to the default aperture), the 180″aperture receives almost twice as much flux than expected from the physical aperture area. At 25 μm the larger apertures see up to 10% more, the smaller ones up to 15% less than expected. At 60 μm the 79″aperture sees 40% more than the default 180″aperture. Within each filter, the sequences on the sky and FCS behave in a similar way. Both sources cause the same deviations from the theoretical prediction. The median (mean) deviations from perfect scaling with aperture area are given in the tables next to the figures.

2.2 Discussion

The FCS signals show a similar pattern as the sky signals, the FCS can therefore be considered as perfectly extended. Previous reports on aperture dependency of FCS illumination (Huth 1997; Huth & Schulz 1997; Laureijs 1996; Schulz et al. 1997) suffered from not linearized signals and are difficult to compare with the findings presented here.
The deviations from “scaling with aperture area” indicate that the apparent solid angles of the apertures are larger than the implemented ones (smaller, if normed signals are less than 1.0). The values in the tables next to the figures give the scaling factors relative to the default apertures.

3 Absolute Photometry on Sky Background

Measurements of the sky background together with a FCS measurement, both in default aperture, have been analysed and compared with COBE-DIRBE results (for a detailed list of observations see Tables 10, 11 and 12 in the appendix). The COBE-DIRBE values have been calculated from the weekly maps, using the median of all DIRBE pixels within 1.5 deg from the nominal position (COBE-DIRBE Explanatory Supplement 1998). The ISOPHOT signal processing was done as described in Appendix C. The signal was then calibrated with the actual response of the detector. Both, COBE-DIRBE and ISOPHOT values, were colour corrected assuming a background blackbody temperature of 275 K. Colour correction values for COBE-DIRBE (ISOPHOT) are: 12.0 μm: 0.93 (0.93), 25.0 μm: 1.31 (1.12) and 60.0 μm: 1.32 (1.09).

Error analysis

Since the background temperatures vary between 259 and 292 K (Ábrahám et al. 1999), the colour correction values have uncertainties of up to 3% for both instruments. The COBE-DIRBE values are given with a sigma of less than 1%, the ISOPHOT signal processing uncertainties are 1 to 5%.

3.1 Results

All 3 ISOPHOT filters show systematic offsets to the COBE values. The offsets are between 10 and 30% at 12 μm, 40 to 60% at 25 μm and about 30% at 60 μm. The offsets for the 12 and 25 μm filters are increasing with absolute surface brightness.

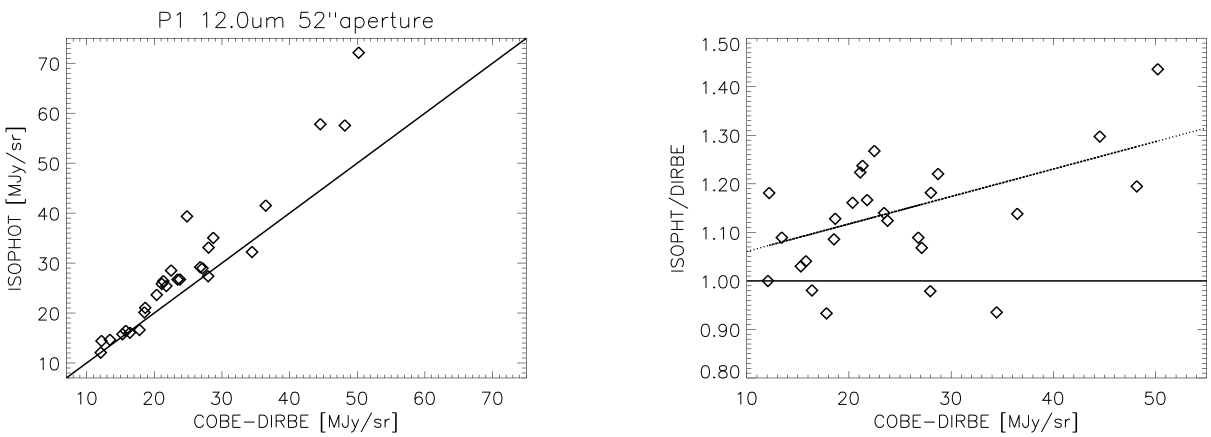

Figure 4: *Colour corrected surface brightness at 12 μm: ISOPHOT vs. COBE-DIRBE.*

3.2 Discussion

The flux dependent offsets in Figures 4 and 5 can be attributed to the signal linearity correction, which is not yet perfect (in fact: no linearization of signals gives excellent results). The offset in Figure 6 is constant, the signal linearization seems to be correct. The systematic offsets between ISOPHOT and COBE-DIRBE are probably due to deviating effective solid angles of the apertures. So far, the effective solid angles are set equal to the physical sizes of the apertures.

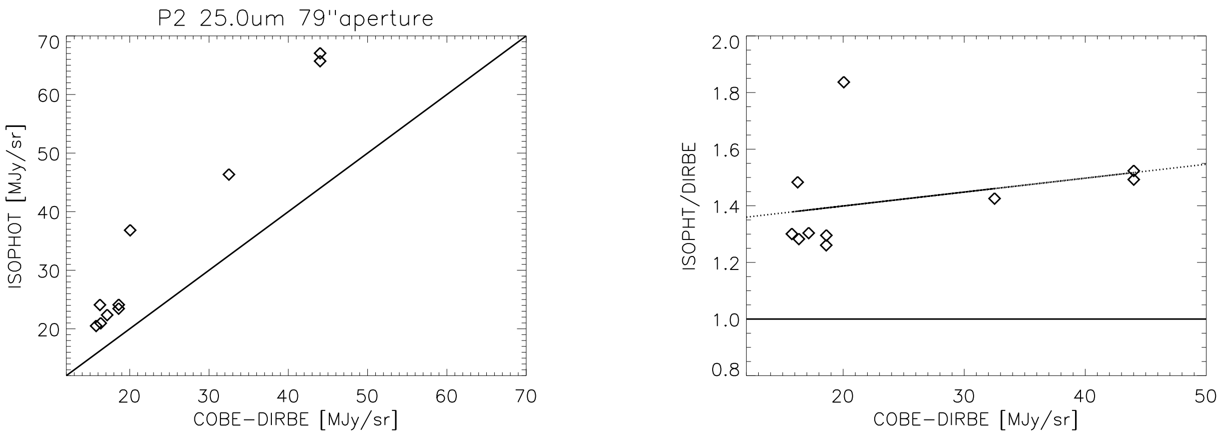

Figure 5: *Colour corrected surface brightness at 25 μm: ISOPHOT vs. COBE-DIRBE.*

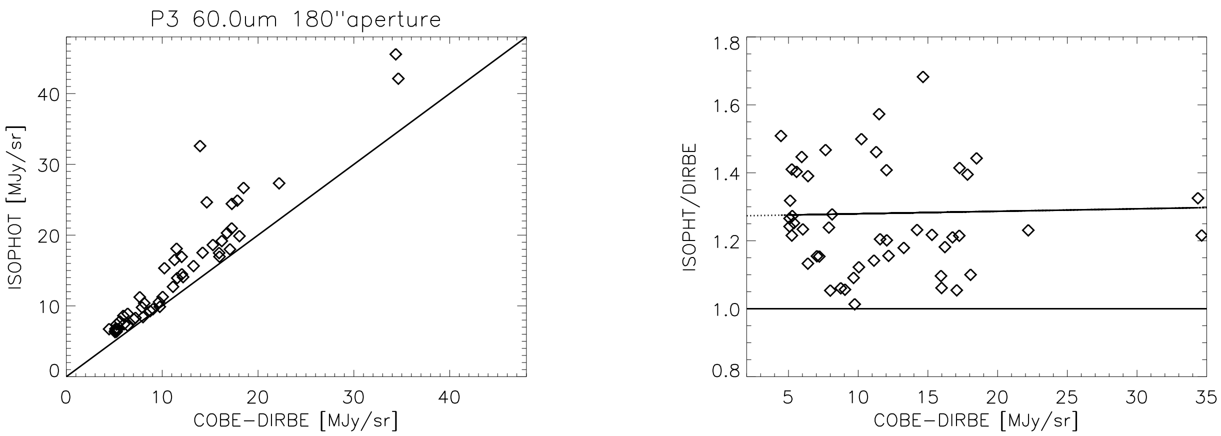

Figure 6: *Colour corrected surface brightness at 60 μm: ISOPHOT vs. COBE-DIRBE.*

Accepting the COBE-DIRBE values as absolute flux reference, the apparent solid angles of PHT are approximately 15% (40%, 30%) larger for the P1-12 μm-52″(P2-25 μm-79″, P3-60 μm-180″) configuration than the ones currently implemented. These offsets can be used, together with the values from the previous chapter, to calculate the effective solid angles for a large range of apertures for all 3 filters.

The offsets and the flux dependencies agree with results by Ábrahám et. al. 2000. They analysed background measurements taken in a large range of filters, but all in the 180″aperture. They also found offsets of 15-20% in case of P1-12 μm and 40-60% in case of P2-25 μm. The slight flux dependency can also be seen in both cases. The P3-60 μm filter was not included in their report. The reason why absolute sky background measurements show the same offsets, independent of aperture, lies in the way the calibration is done: Both, sky and FCS are taken in the same aperture and the erroneous solid angles cancels out. What is left, is the error in the solid angle of the default aperture which connects the point-source calibration to extended source calibration.

4 Relative Aperture Sequences on Point-sources

Aperture sequences on different stars have been analysed. First the background contribution was determined from the 2 largest apertures and then subtracted in all apertures accordingly (see Müller 2000b for details of the method). The pure point-source signal was then divided by the theoretical f_{psf} values (see Table 6 in Appendix A) and normalized to the 180″aperture. If theoretical and measured point-spread-functions agree, all calculated signal ratios should be close to 1.

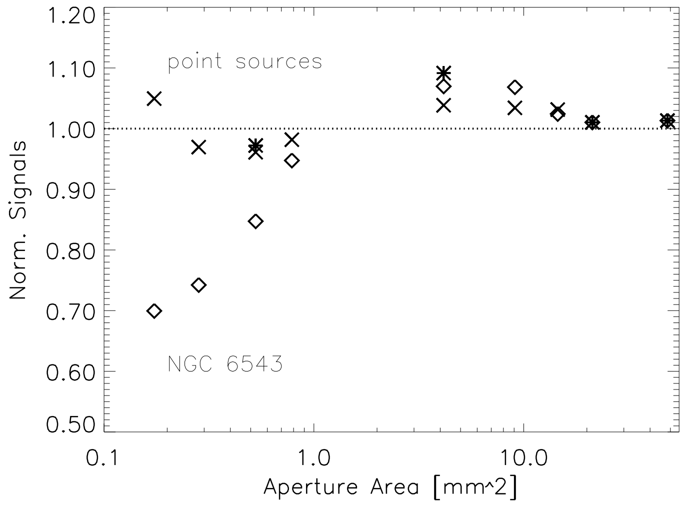

Figure 7: *P1, 12 μm: Background subtracted source signals, divided by the f_{psf} values and normalized to the 180″ aperture.*

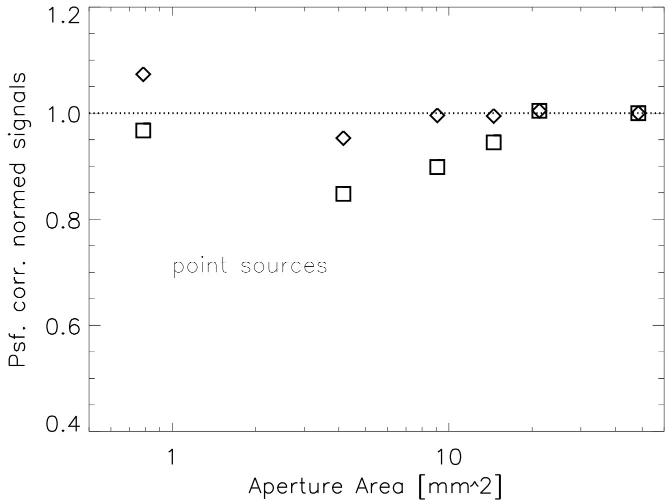

Figure 8: *P2, 25 μm: Background subtracted source signals, divided by the f_{psf} values and normalized to the 180″ aperture.*

4.1 Results

At 12 μm the signals follow nicely the theoretical predictions down to the 18″aperture. NGC 6543 deviates in the smallest apertures which shows that this source is extended. NGC 6090 had to be excluded, because the background determination from the 2 largest apertures failed. At 25 μm the signals follow the prediction. Unfortunately no measurements at smaller apertures

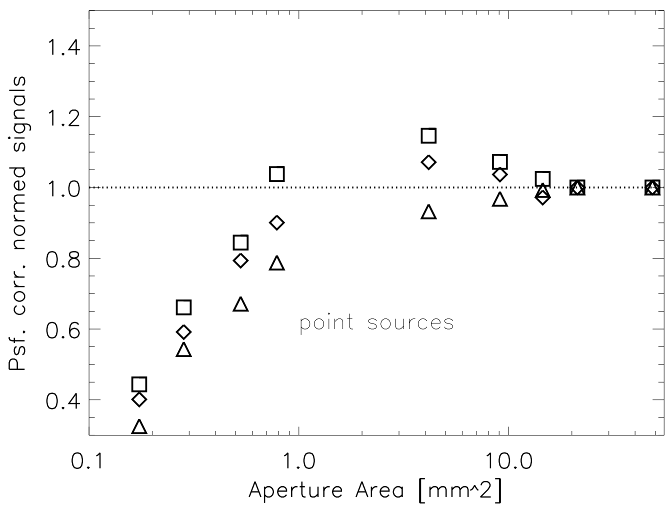

Figure 9: *P3, 60 μm: Background subtracted source signals, divided by the f_{psf} values and normalized to the 180″ aperture.*

exist. At 60 μm the signals follow the predictions for the aperture range from 23″to 180″, but strongly deviate for smaller apertures.

4.2 Discussion

Point-source signals behave as expected for the aperture range between 23″and 180″. Example: Theoretically, 93% of a point-source flux lies within the P3, 60 μm 180″aperture and only 46% within the 23″aperture. This is confirmed by the above measurements. The same is valid for the aperture range from 10″to 180″for P1 12 μm and from 23″to 180″for P2 25 μm: The measured fractions of source fluxes are following the theoretical calculations. Deviations can only been seen at apertures 18″and smaller in the P3 60 μm configuration (see Figure 4). A recalculation of f_{psf} values by Müller (2000b) gave up 6% different values from the ones currently implemented in PIA V9.0.1(e).

5 Absolute Photometry on Point-sources

The calibration of ISOPHOT is based on measurements of celestial photometric standards against the FCS in default apertures. But how does the point-source photometry in non-default apertures look like? How can one combine the results from the peculiar behaviour of the aperture sequences on the sky and the FCS with the almost ideal point-source behaviour?

In the following different aspects of the measurement sequences are considered: First, the backgrounds are analysed to check if the results found before in Section 3 are confirmed. Second, the measurement sequences as a whole are analysed. The background subtraction was always done at the signal level. The "on-minus-off" signals were then calibrated with the corresponding FCS measurements.

5.1 Background analysis

For all measurement sequences the absolute value of the background was determined with the corresponding FCS measurement in the same aperture. The individual values are given, together with details about the measurement sequences, in Tables 13, 14 and 15 in the Appendix.

The comparisons with COBE-DIRBE show similar offsets as they were found in Section 3. Also the signal linearization problem for P2 25 μm appears again, this time it shows up as a dependency of the aperture area. The results per filter:

- For P1 12 μm the ratios are systematically larger than one (Median: 1.32). A clear trend with aperture area can not be seen.
- For P2 25 μm the ratios are systematically larger than one (Median: 1.59). Here, also trend with aperture area can be seen: PHT/COBE ratios are 1.35 (52$''$), 1.41 (79$''$), 1.65 (120$''$), 1.81 (180$''$). This dependency is probably due to the incorrect signal linearization: With increasing apertures the signal value increases and therefore the linearization changes.
- For P3 60 μm the PHT/COBE ratios are systematically larger than one (1.27 $\pm$ 0.13). A clear trend with aperture area can not be seen.

In the following the background has always been subtracted on signal level.

5.2 At 12 μm

The background signal has been subtracted from the on-source signal on SCP level. The pure point-source signal has then been calibrated against the FCS, taken in the same aperture. For the TDTs of the measurements see Appendix D.

The flux of the 2 stars varies a factor of 2, depending on the aperture. This confirms the results from Figure 1, where the 180$''$aperture signals are a factor 2 larger than expected. Here, the responsivities derived from the 180$''$FCS measurements are a factor of 2 larger than the ones in the 52$''$aperture. The leads to the low fluxes for large apertures.

Source	<52″>	79″	180″	Comparison
HR 7341	0.83(2)	0.75(2)	0.42(1)	PH model flux 0.94 ± 0.03 Jy
HR 7310	11.75(1)	—	6.80(1)	PH model flux 14.49 ± 0.45 Jy

Table 1: *Colour corrected point-source fluxes (number of measurements) in [Jy] at 12 μm in different apertures. PH: P. Hammersley models.*

5.3 At 25 μm

The background signal has been subtracted from the on-source signal on SCP level. The pure point-source signal has then been calibrated against the FCS, taken in the same aperture. For the TDTs of the measurements see Appendix D.

Source	52″	<79″>	120″	180″	Comparison
HR 7341	—	0.20(1)	—	0.44(1)	PH model flux 0.22 ± 0.01 Jy
HR 7310	—	3.27(3)	4.20(2)	4.84(1)	PH model flux 3.41 ± 0.13 Jy
HR 6132	—	—	5.01(1)	5.68(1)	PH model flux 3.80 ± 0.12 Jy
HR 7854	0.27(1)	0.20(1)	—	—	PH model flux 0.19 ± 0.01 Jy
HR 0794	—	—	—	2.06(3)	cc IRAS flux 1.63 ± 0.10 Jy

Table 2: *Colour corrected point-source fluxes (number of measurements) in [Jy] at 25 μm in different apertures. PH: P. Hammersley models; cc: colour corrected.*

Here, again a clear trend of the stellar fluxes with aperture area can be seen. From Figures 2 and 5 one would not expect this strong variations, but the influence of the wrong linearity correction and/or the different apparent solid angles (40 to 60% differences between COBE and ISOPHOT) are most likely causing the strong deviations.

5.4 At 60 μm

The background signals have been subtracted from the on-source signals on SCP level. The pure point-source signals have then been calibrated against the FCS, taken in the same aperture. For the TDTs of the measurements see Appendix D.

Source	79″	99″	120″	<180″>	Comparison
HR 5340	—	19.12(1)	—	20.59(1)	PH model flux 21.0 ± 1.3 Jy
HR 7310	—	0.58(2)	—	0.61(2)	PH model flux 0.59 ± 0.03 Jy
HR 0165	1.48(1)	—	1.64(1)	1.93(1)	cc IRAS flux 1.86 ± 0.22 Jy
HR 7980	1.26(1)	—	—	1.56(1)	cc IRAS flux 1.14 ± 0.10 Jy

Table 3: *Colour corrected point-source fluxes (number of measurements) in [Jy] at 60 μm in different apertures. PH: P. Hammersley models; cc: colour corrected.*

The fluxes in smaller apertures are significantly lower than in the default 180″aperture. In the 79″aperture HR0165 has 23% less and HR7980 19% less than in the 180″. The signal/responsivity overestimation can clearly be seen.

5.5 Discussion

Assume an off-source, an on-source and a FCS measurement in the same non-default aperture, for example P3, 60 μm, 79″aperture. We subtract the off- from the on-source on signal level (SCP). The pure source signal will then be calibrated against the FCS. According to Figure 3 the FCS signal will be 39% higher than expected. This means that the responsivity will also be 39% higher than a comparable FCS measurement in the 180″aperture (see Appendix B for the formula). Figure 4 shows a normal behaviour for point-sources between the 79″and the 180″aperture. Therefore, the point-source signal should be as expected for the 79″aperture. The 39% higher responsivity would lead to a 39% **lower** flux.

In practice, the lower fluxes are confirmed (see Table 3), but the effect is not as strong as predicted. Both stars have approximately 20% lower flux in the 79″than in the 180″aperture. The fluxes in the default apertures agree with models and/or IRAS fluxes within the calibration uncertainties (Schulz et al. 1999). The differences are for P1 12 μm: 12% (HR 7341), 19% (HR 7310), P2 25 μm: 10% (HR 7341), 4% (HR 7310), 5% (HR 7854), P3 60 μm: 23% (HR 7310), 4% (HR 0165) and 37% (HR 7980).

6 Conclusions

Based on the analysis of 3 ISOPHOT filters, the following conclusions are drawn:

- The FCS is flat, FCS signals show the same trends as background signals.
- ISOPHOT photometry of point-sources in default apertures works fine (see also Schulz et al. 1999, Table 3 for statistical analysis), in non-default apertures it is problematic.
- Comparison between ISOPHOT and COBE photometry indicates that the apparent solid angles of the PHT apertures are larger the currently implemented ones (10-50% for the default apertures and up to a factor of 2 for some non-default apertures).
- The 25 μm filter still shows signal linearity problems of the order of 30% in the brightness range from 15 to 50 MJy/sr.
- The theoretical f_{psf} values for point-sources are confirmed for the aperture range from 23″to 180″. For smaller apertures the measured values deviate.

These results have further consequences:

- The default response is strongly biased towards the default aperture, which is most frequently used. This means it is not applicable in non-default apertures.
- Extended sources lie between the two extreme behaviours of sky measurements (perfectly extended) and point-sources. To obtain reliable photometry, the default aperture as well as non-default aperture measurements have to be analysed carefully and the trends, offsets and uncertainties estimated correspondingly.
- Faint point-sources on a strong background fall under the category of sky background measurements, where the solid angles are more important than for bright sources. Photometry in non-default apertures has to be handled with care.
- The combination of on-source and off-source measurements in different apertures is difficult and strongly affected by the wrong solid angles.

- Aperture sequences on strongly structured extended sources will be extremely difficult to analyse. On the other hand, aperture sequences can be used to distinguish between point- and extended sources (Müller 2000b). It is also possible to determine quantitatively the source extension from PHT04 sequences, in excellent agreement with ISOCAM results (Siebenmorgen et al. 2000).

7 Acknowledgements

PIA is a joint development by the ESA Astrophysics Division and the ISOPHOT consortium. I would like to thank Rene Laureijs, Bernhard Schulz, Peter Ábrahám and Ulrich Klaas for many helpful discussions. Peter Ábrahám also provided a tool to extract surface brightness values from the COBE-DIRBE weekly maps.

References

[1] Ábrahám P., Leinert C. Acosta–Pulido J.A., Schmidtobreick L and Lemke D. 1999, ESA SP-427, Cox & Kessler (Eds.), 145

[2] Ábrahám P., Héraudeau P. & Klaas U., “Comparison of the ISOPHOT and COBE/DIRBE Absolute Photometry in low Surface Brightness regions”, Version 1.0, ISO internal report, 21-Jul-2000.

[3] “COBE Diffuse Infrared Background Experiment (DIRBE) Explanatory Supplement”, Version 2.3, Hauser M.G., Kelsall T., Leisawitz D. and Weiland J. (Eds.), COBE Ref. Pub. No. 98-A (Greenbelt, MD: NASA/GSFC), available in electronic form from the NSSDC, 1998

[4] Huth S. & Schulz B., “P1-Aperture Dependency of FCS Illumination”, ISOPHOT internal report 1997.

[5] Huth S. “P3 Aperture Dependency of FCS Illumination”, ISOPHOT internal report 1997.

[6] Laureijs R.J. “Analysis P3 Aperture Sequence”, ISOPHOT internal report 1996.

[7] Müller T.G., “ISOPHOT Aperture Profiles and Background Measurements”, ISO beyond point sources: studies of extended infrared emission, Proceedings, ESA SP-453, Laureijs, Leech & Kessler (Eds.), 2000a.

[8] Müller T.G., “ISOPHOT Aperture Sequences on Point- and Extended Sources”, ISO beyond point sources: studies of extended infrared emission, Proceedings, ESA SP-453, Laureijs, Leech & Kessler (Eds.), 2000b.

[9] Schulz B., Lu N. & Huth S., “P2 Aperture Dependency of FCS Illumination”, ISOPHOT internal report 1997.

[10] Schulz B., Huth S., Kinkel U. et al. 1999, ESA SP-427, Cox & Kessler (Eds.), 89.

[11] Siebenmorgen R., Prusti T., Natta A. & Müller T.G. 2000, A&A accepted.

A Used Values

A.1 Aperture Areas, Solid Angles and Default Apertures

Name	Area [mm^2]	Solid Angle [$\times$ 10^{-7} sr]
5″	0.0314	0.00388
7.6″	0.1001	0.01236
10″	0.1735	0.02142
13.8″	0.2827	0.03491
18″	0.5281	0.06251
23″	0.7854	0.09696
20x32″	1.1288	0.13940
52″	4.1548	0.51290
79″	9.0792	1.12090
99″	14.5220	1.79280
120″	21.2372	2.62190
127x127″	30.2500	3.73460
180″	48.3982	5.97510

Table 4: *Apertures areas and their Solid Angles, taken from* `PPOMEGA.FITS`.

Detector	Filter	Aperture
P1	12.0	52″
P2	25.0	79″
P3	60.0	180″

Table 5: *Default apertures.*

A.2 Point-Spread-Function Values

Filter	Apertures 10″	13.8″	18″	23″	52″	79″	99″	120″	180″
P1_12	0.69	0.79	0.90	0.90	0.95	0.97	0.98	0.98	0.99
P2_25	0.53	0.64	0.68	0.69	0.90	0.93	0.95	0.96	0.97
P3_60	0.14	0.22	0.35	0.46	0.69	0.85	0.90	0.90	0.93

Table 6: *Point-spread-function values f_{psf}, taken from* `PPSF.FITS` *for 3 filters.*

B Responsivity and Flux Determination

B.1 Responsivity Calculation

$$R = \frac{S_{FCS} C}{P_{FCS} F f} \tag{1}$$

with S_{FCS}: the measured FCS signal
C: capacitance,
P_{FCS}: the inband-power provided by the FCS, directly connected to the applied heating power and based on standard source measurements.
Ff: Filter to filter / Flat-field factor corresponding to the pixel and filter used.

B.2 Flux Density and Surface Brightness

The inband-power calculation for scientific targets is done in the following way:

$$P = \frac{S_{src} \times C}{R_{actual}} \qquad [W] \tag{2}$$

with S_{src}: signal from the sky source
C: capacitance,
R_{actual}: actual detector responsivity

Flux density [Jy] and surface brightness [MJy/sr] are then calculated with:

$$\begin{aligned} F_\nu &= \frac{P}{C1 \times f_{psf}} \qquad [Jy] \qquad (P1, P2, P3) \\ F_\nu &= \frac{P}{C1} \qquad [Jy/beam] \qquad (C100, C200) \\ &and \\ B_\nu &= \frac{P}{C1 \times OBS \times \Omega} \qquad [MJy/sr] \end{aligned}$$

With C1: a constant per detector
f_{psf}: the point spread function corresponding to detector, filter and aperture used
OBS: an obscuration factor of the secondary mirror of the ISO telescope (OBS=0.91)
Omega: the solid angle of the aperture or array projected on the sky.

C Data Reduction

```
Signal processing with PIA V9.0.1(e) from ERD to SCP.

General Batch Processing from ERD to SCP:
* Standard Choices for Read-Outs
* Standard Choices for Signal selection, but discarding
  the first half of the signals
* ERD corrections: - ramp linearization
                   - ramps deglitching (single & 2 threshold)
* SRD corrections: - reset interval correction
                   - dark current subtraction (one value per data point)
                   - signal linearization
                   - signal deglitching (2 iterations, min/max clip)
* SCP corrections: - none
```

D Observations

Table 7: *Aperture Sequences on Sky Background.*

TDT	PROPID	DATE	AOT	Aperture Observation Sequence
		P1 12 μm Aperture Sequences on Sky Background		
71301102	52512003	28-Oct-97	P04	10,13.8,18,23,52
71301103	52512003	28-Oct-97	P04	52,79,99,120,180
07307701	52512_P1	29-Jan-96	P99	10,13.8,18,20x32,23,52,79,99,120,127x127,180
07307802	52512_P1	29-Jan-96	P99	127x127,120,99,79,52,23,–,18,13.8,10
		P2 25 μm Aperture Sequences on Sky Background		
71301204	52512003	28-Oct-97	P04	79,99,120,180
72002401	5412P204	05-Nov-97	P04	23,52,79,99,120,180
80500701	P04PSF01	28-Jan-98	P04	23,52,79,99,120,180
07700401	52512_P2	02-Feb-96	P99	18,20x32,23,52,79,99,120,127x127,180
07700502	52512_P2	02-Feb-96	P99	127x127,120,99,79,52,23,20x32,18
		P3 60 μm Aperture Sequences on Sky Background		
71302105	52512003	28-Oct-97	P04	79,99,120,180
79600205	P04PSF01	19-Jan-98	P04	23,52,79,99,120,180
80501507	P04PSF01	28-Jan-98	P04	18,23,52,79,99,120,180
81500709	P04PSF01	07-Feb-98	P04	10,13.8,18,23,52,79,99,120,180

Table 8: *Aperture Sequences on FCS (all P99 AOT). Remarks: 1) Some TDTs appear twice, because the sequences consisted of switching between FCS1, sky and FCS2. The FCS2 signals are usually strong drifting and therefore not usable. 2) The on-sky measurement TDT 07307802 in the 20x32 aperture was not performed. 3) The pointing on HR 7980, measurement TDT 72002402, was off by 4.2 arcmin and had to be excluded. 4) The aperture sequences of TDTs 85303101 and 85303202 have been sorted by heating power.*

TDT	PROPID	DATE	FCS	Aperture Observation Sequence
		P1 12 μm Aperture Sequences on FCS		
04103501	52402AP1	28-Dec-95	FCS1	18,23,20x32,52,79,99,120,127x127, 180,127x127,120,99,79,52,20x32,23,18
06507301	52402_P1	21-Jan-96	FCS1	5,7.6,10,13.8,18,23,20x32,52,79,99, 120,127x127,180,127x127,120,99,79, 52,20x32,23,18,13.8,10,7.6,5
07307701	52512_P1	29-Jan-96	FCS1/2	10,13.8,18,20x32,23,52,79,99,120,127x127,180
07307802	52512_P1	29-Jan-96	FCS1/2	127x127,120,99,79,52,23,20x32,18,13.8,10
		P2 25 μm Aperture Sequences on FCS		
06701703	52402AP2	23-Jan-96	FCS1	18,23,20x32,52,79,99,120,127x127,180
06701804	52402AP2	23-Jan-96	FCS1	127x127,120,99,79,52,20x32,23,18
07700401	52512_P2	02-Feb-96	FCS1/2	18,20x32,23,52,79,99,120,127x127,180
07700502	52512_P2	02-Feb-96	FCS1/2	127x127,120,99,79,52,23,20x32,18
		P3 60 μm Aperture Sequences on FCS		
02902001	52402_P3	16-Dec-95	FCS1	52,79,99,120,127x127,180
02902102	52402_P3	16-Dec-95	FCS1	127x127,120,99,79,52
85303101	242P301	17-Mar-98	FCS1	52,79,99,120,180 (3×)
85303202	242P301	17-Mar-98	FCS1	52,79,99,120,180 (3×)

Table 9: *Aperture Sequences on Point-Sources.*

TDT	PROPID	DATE	AOT	Aperture Observation Sequ.	Source
		P1 12 μm Aperture Sequences on Point-Sources			
01301302	P_JITT1	30-Nov-95	P04	7.6,10,13.8,18,23,52,79,99,120,180	NGC 6090 (extended)
01301402	P_JITT2	30-Nov-95	P04	7.6,10,13.8,18,23,52,79,99,120,180	NGC 6090 (extended)
05702402	AOTPVP06	13-Jan-96	P04	10,13.8,18,23,52,79,99,120,180	NGC 6543 (extended)
05702506	AOTPVP06	13-Jan-96	P04	10,13.8,18,23,52,79,99,120,180	HR 6705
78000601	PAW_2	03-Jan-98	P04	10,18,52,120,180	03287-1535
		P2 25 μm Aperture Sequences on Point-Sources			
06101501	AOTPVP6B	17-Jan-96	P04	23,52,79,99,120,180	HR 6705
72002402	5412P204	05-Nov-97	P04	23,52,79,99,120,180	HR 7980 (4.2' offset)
80500702	P04PSF01	18-Jan-98	P04	23,52,79,99,120,180	HR 617
		P3 60 μm Aperture Sequences on Point-Sources			
79600206	P04PSF01	19-Jan-98	P04	10,13.8,18,23,52,79,99,120,180	HR 6705
80501508	P04PSF01	28-Jan-98	P04	10,13.8,18,23,52,79,99,120,180	HR 337
81500710	P04PSF01	07-Feb-98	P04	10,13.8,18,23,52,79,99,120,180	HR 1457

Table 10: *P1 12 μm Absolute Photometry on Sky Background: Observations and colour corrected surface brightness.*

TDT	RA	Dec	Date	COBE-DIRBE [MJy/sr]	ISOPHOT [MJy/sr]
30801917	19h07m07.40s	-23d21'22.6"	20-Sep-96	29.16	31.15
31601909	03h33m11.10s	+64d45'48.7"	28-Sep-96	19.15	17.87
35602101	17h57m19.00s	+51d26'31.1"	07-Nov-96	16.45	16.95
42600403	17h17m40.30s	+37d20'29.0"	15-Jan-97	19.94	21.65
47600205	17h58m33.72s	+66d43'05.2"	06-Mar-97	14.45	15.74
47600413	15h34m57.52s	+23d35'17.5"	06-Mar-97	16.98	17.67
47600509	16h52m58.81s	+02d19'09.6"	06-Mar-97	25.57	28.74
48801730	03h22m09.60s	+64d42'31.6"	18-Mar-97	22.94	28.38
48801731	03h33m11.10s	+64d45'48.7"	18-Mar-97	22.70	27.77
56100120	13h00m09.21s	+20d33'52.1"	30-May-97	20.06	22.63
64401532	12h33m54.90s	-62d46'57.0"	21-Aug-97	28.81	31.38
67601731	18h29m52.77s	+01d16'19.8"	21-Sep-97	25.20	28.73
67900660	04h14m48.00s	+27d55'05.1"	24-Sep-97	30.06	29.43
67901250	04h21m59.30s	+19d29'36.8"	25-Sep-97	30.13	35.60
70704638	18h05m37.36s	+02d30'02.6"	23-Oct-97	37.04	34.65
70704809	18h55m11.48s	-22d40'10.9"	23-Oct-97	53.99	77.54
71001253	16h16m46.58s	+67d11'51.5"	25-Oct-97	13.12	15.49
71700837	17h12m21.75s	+45d39'29.5"	01-Nov-97	17.62	17.28
73201101	22h10m15.66s	+06d12'14.3"	16-Nov-97	24.18	30.66
78001221	06h19m49.30s	-64d23'42.3"	04-Jan-98	12.99	12.99
79601903	03h28m09.00s	-01d19'16.6"	20-Jan-98	23.42	27.32
82100252	16h55m38.90s	-08d20'26.8"	13-Feb-98	47.89	62.14
83700411	17h19m01.93s	-34d59'28.0"	01-Mar-98	51.78	61.87
83802203	05h16m55.68s	+46d00'05.8"	03-Mar-98	26.70	42.31
84200640	17h30m33.82s	-01d03'54.1"	06-Mar-98	30.88	37.69
86603031	05h02m11.90s	+43d49'39.8"	30-Mar-98	39.22	44.63
86900508	17h48m03.60s	+02d42'22.9"	02-Apr-98	21.89	25.42

Table 11: *P2 25 μm Absolute Photometry on Sky Background: Observations and colour corrected surface brightness.*

TDT	RA	Dec	Date	COBE-DIRBE [MJy/sr]	ISOPHOT [MJy/sr]
07700401	14h07m15.80s	-07d15'49.0"	02-Feb-96	44.01	67.05
07700502	14h07m15.80s	-07d15'49.0"	02-Feb-96	44.01	65.70
35300303	17h57m19.00s	+51d26'31.1"	03-Nov-96	18.60	23.45
35602406	17h57m19.00s	+51d26'31.1"	07-Nov-96	18.61	24.11
47600205	17h58m33.72s	+66d43'05.2"	06-Mar-97	17.15	22.36
47600509	16h52m58.81s	+02d19'09.6"	06-Mar-97	32.51	46.35
69900501	19h18m39.70s	+49d31'10.6"	14-Oct-97	16.24	24.09
70705711	06h44m52.38s	-16d38'09.2"	23-Oct-97	20.05	36.83
71300501	19h36m31.50s	+50d10'21.8"	28-Oct-97	16.34	20.96
76602302	05h48m17.10s	-51d03'59.5"	21-Dec-97	15.76	20.50

Table 12: *P3 60 μm Absolute Photometry on Sky Background: Observations and colour corrected surface brightness.*

TDT	RA	Dec	Date	COBE-DIRBE [MJy/sr]	ISOPHOT [MJy/sr]
08400326	11h08m03.50s	-77d54'17.5"	09-Feb-96	5.58	7.83
08402043	15h24m19.80s	-23d00'39.9"	09-Feb-96	17.27	24.43
08500517	15h48m10.40s	+28d09'23.9"	10-Feb-96	6.40	8.90
08500731	15h27m47.10s	+19d27'44.0"	10-Feb-96	7.66	11.24
09100504	17h31m25.00s	-23d51'45.6"	16-Feb-96	34.37	45.56
10401745	15h15m48.40s	-37d15'16.4"	29-Feb-96	10.23	15.34
10402180	15h41m11.45s	-44d33'38.8"	29-Feb-96	12.03	16.94
10402325	15h39m46.50s	-42d29'54.6"	29-Feb-96	11.50	18.09
10402665	16h06m58.00s	-27d49'10.0"	29-Feb-96	18.49	26.68
10601105	18h37m36.13s	+38d58'00.1"	02-Mar-96	5.95	8.61
12100842	19h04m24.19s	-05d47'05.5"	17-Mar-96	22.20	27.33
13101190	19h52m30.10s	+22d21'14.3"	27-Mar-96	13.95	32.60
13601440	18h24m29.79s	-29d52'50.4"	01-Apr-96	17.84	24.89
14201506	20h24m21.39s	+42d11'12.3"	07-Apr-96	130.65	188.47
15900606	20h24m21.39s	+42d11'12.3"	24-Apr-96	133.91	175.62
16402915	22h58m19.01s	-29d43'12.5"	29-Apr-96	11.57	13.94
16900508	09h39m54.00s	+12d04'54.0"	04-May-96	15.94	17.48
18401560	11h49m03.73s	+14d34'19.8"	19-May-96	12.05	14.48
18600323	22h35m27.59s	-17d09'28.0"	21-May-96	16.77	20.30
24001020	11h23m01.72s	-24d36'40.9"	14-Jul-96	10.05	11.28
26300813	23h58m24.77s	+51d29'18.8"	05-Aug-96	6.39	7.24
28200975	00h09m10.47s	+59d14'59.8"	24-Aug-96	11.13	12.71
29701056	14h36m08.00s	-39d27'33.0"	08-Sep-96	13.27	15.65
30200833	17h56m23.29s	+58d07'06.4"	13-Sep-96	4.46	6.73
33701833	21h38m51.90s	-30d04'14.2"	19-Oct-96	11.29	16.50
35300305	17h57m19.00s	+51d26'31.1"	03-Nov-96	5.24	6.37
35300715	22h58m19.02s	-29d43'12.6"	03-Nov-96	9.67	10.55
35602507	17h57m19.00s	+51d26'31.1"	07-Nov-96	5.27	6.71
35700413	12h45m07.80s	+45d32'25.0"	07-Nov-96	6.03	7.44
35700825	19h50m33.91s	+33d00'51.3"	07-Nov-96	14.22	17.52
36000802	01h04m16.22s	-73d48'17.0"	10-Nov-96	5.12	6.75
36802047	22h19m27.90s	+59d45'22.0"	18-Nov-96	17.25	20.96
39300930	01h34m37.78s	-15d34'34.9"	13-Dec-96	9.05	9.56
39301185	01h44m04.46s	-15d50'17.5"	14-Dec-96	8.75	9.28
40101835	02h45m06.13s	-18d40'21.4"	22-Dec-96	7.21	8.32
41700945	15h48m10.40s	+28d09'23.9"	06-Jan-97	7.04	8.13
41905011	17h44m55.50s	+49d56'39.8"	08-Jan-97	5.24	7.39
42604805	21h43m30.40s	+58d52'48.1"	16-Jan-97	14.65	24.65
43306021	01h33m51.30s	+62d32'52.0"	22-Jan-97	12.18	14.08
45200201	14h15m39.70s	+19d15'57.0"	10-Feb-97	7.90	9.79
45602028	17h31m25.00s	-23d51'45.6"	14-Feb-97	34.64	42.12
49302621	19h16m06.80s	-33d31'20.4"	23-Mar-97	15.98	16.96
60700418	12h43m50.80s	-54d16'25.0"	14-Jul-97	9.75	9.88
60900104	14h57m25.18s	-63d34'24.4"	16-Jul-97	16.22	19.17
62402210	05h48m12.10s	-50d54'04.6"	01-Aug-97	5.39	6.75
62900501	14h15m42.40s	+19d13'52.7"	06-Aug-97	8.13	10.39
63602297	05h19m41.40s	+05d44'42.1"	13-Aug-97	15.29	18.62
67801001	17h56m36.90s	+51d26'20.3"	23-Sep-97	5.08	6.43
67801110	17h56m36.90s	+51d26'20.3"	23-Sep-97	5.08	6.31
69301906	06h44m34.80s	+25d25'57.5"	09-Oct-97	17.07	18.00
71101029	19h15m23.40s	-06d56'50.0"	26-Oct-97	18.06	19.87
79601208	03h32m55.93s	-09d21'29.7"	20-Jan-98	8.00	8.43

Table 13: *P1 12 μm absolute photometry of point-sources in non-default apertures. Some of the measurements (1) show strong transients. For background measurements the calibrated and colour corrected ISOPHOT and COBE-DIRBE values are given together with the ratio.*

TDT	PROPID	AOT	Aper [″]	Target	$COBE_{cc}$ [MJy/sr]	PHT_{cc} [MJy/sr]	PHT/COBE
03703102-1	52401H03	P99	52	FCS1 0.0 mW			
03703102-2	52401H03	P99	52	HR 7341 on			
03703102-3	52401H03	P99	52	FCS1 3.52 mW			
03703102-4	52401H03	P99	52	HR 7341 on			
03703102-5	52401H03	P99	52	FCS1 3.74 mW			
03703102-6	52401H03	P99	52	HR 7341 on			
03703102-7	52401H03	P99	52	FCS1 3.99 mW			
03703102-8	52401H03	P99	52	HR 7341 on			
03703102-9	52401H03	P99	52	FCS1 4.57 mW			
03703102-10	52401H03	P99	52	HR 7341 on			
03703102-11	52401H03	P99	52	FCS1 0.00 mW			
03703203-1	52401H03	P99	52	HR 7341 off	16.71	18.01	1.08
20303303-1	5241PA20	P99	52	HR 7341 off	12.78	16.89	1.32
20303404-1	5241PA20	P99	52	FCS1 0.00 mW			
20303404-2	5241PA20	P99	52	FCS1 4.16 mW			
20303404-3	5241PA20	P99	52	HR 7341 on			
69900401-3	CFREP104	P03	79	HR 7341 off	13.54	14.46	1.07
69900401-4	CFREP104	P03	79	FCS1 4.16 mW			
69900402-3	CFREP104	P03	79	HR 7341 on			
69900402-4	CFREP104	P03	79	FCS1 4.16 mW			
81800505-1	5242AS01	P03	180	FCS1 3.96 mW			
81800505-2	5242AS01	P03	180	HR 7341 3×2 nodding	18.24	15.89	0.87
81800505-3	5242AS01	P03	180	FCS1 3.96 mW			
11201407-1[1]	5241PA01	P99	52	HR 7310 off	15.16	32.99	2.18
11201508-1	5241PA01	P99	52	FCS1 0.00 mW			
11201508-2	5241PA01	P99	52	FCS1 4.91 mW			
11201508-3[1]	5241PA01	P99	52	HR 7310 on			
81802011-1	5242AS01	P03	180	FCS1 4.40 mW			
81802011-2	5242AS01	P03	180	HR 7310 3×2 nodding	15.32	21.95	1.43
81802011-3	5242AS01	P03	180	FCS1 4.40 mW			

Table 14: *P2 25 μm absolute photometry of point-sources in non-default apertures. Some of the measurements (1) show strong transients. For background measurements the calibrated and colour corrected ISOPHOT and COBE-DIRBE values are given together with the ratio.*

TDT	PROPID	AOT	Aper ["]	Target	$COBE_{cc}$ [MJy/sr]	PHT_{cc} [MJy/sr]	PHT/COBE
20304701-1[1]	5241PB06	P99	79	HR 7341 off	15.50	20.31	1.31
20304802-1[1]	5241PB06	P99	79	HR 7341 on			
20304802-2[1]	5241PB06	P99	79	FCS1 1.51 mW			
20304802-3[1]	5241PB06	P99	79	FCS1 1.61 mW			
69900501-2	CFREP204	P03	79	HR 7341 off	16.24	24.09	1.48
69900501-3	CFREP204	P03	79	FCS1 1.53 mW			
69900502-2	CFREP204	P03	79	HR 7341 on			
69900502-3	CFREP204	P03	79	FCS1 1.53 mW			
82500702-4	5242AS02	P03	180	FCS1 1.42 mW			
82500702-5	5242AS02	P03	180	HR 7341 3×2 nodding	19.98	36.03	1.80
82500702-6	5242AS02	P03	180	FCS1 1.42 mW			
03310501-1	52401L03	P99	79	HR 7310 off	16.59	23.03	1.39
03310602-1	52401L03	P99	79	FCS1 0.00 mW			
03310602-2	52401L03	P99	79	HR 7310 on			
03310602-3	52401L03	P99	79	FCS1 1.50 mW			
03310602-4	52401L03	P99	79	HR 7310 on			
03310602-5	52401L03	P99	79	FCS1 1.75 mW			
03310602-6	52401L03	P99	79	HR 7310 on			
03310602-7	52401L03	P99	79	FCS1 1.88 mW			
03310602-8	52401L03	P99	79	HR 7310 on			
03310602-9	52401L03	P99	79	FCS1 2.04 mW			
03310602-10	52401L03	P99	79	HR 7310 on			
03310602-11	52401L03	P99	79	FCS1 0.00 mW			
03310703-1	52401L03	P99	79	HR 7310 off	16.59	22.31	1.35
11203003-1	5241PB01	P99	79	HR 7310 off	17.73	23.43	1.32
11203104-1	5241PB01	P99	79	FCS1 0.00 mW			
11203104-2	5241PB01	P99	79	FCS1 1.62 mW			
11203104-3	5241PB01	P99	79	HR 7310 on			
44004201-1	5241PB20	P99	79	HR 7310 off	17.44	25.32	1.45
44004302-1	5241PB20	P99	79	FCS1 0.00 mW			
44004302-2	5241PB20	P99	79	FCS1 1.86 mW			
44004302-3	5241PB20	P99	79	FCS1 1.72 mW			
44004302-4	5241PB20	P99	79	HR 7310 on			
74800609-1	CFAINT31	P03	120	FCS1 1.53 mW			
74800609-2	CFAINT31	P03	120	HR 7310 3×2 nodding	14.23	24.68	1.73
74800609-3	CFAINT31	P03	120	FCS1 1.53 mW			
76201511-1	CFAINT32	P03	120	FCS1 1.53 mW			
76201511-2	CFAINT32	P03	120	HR 7310 3×2 nodding	16.45	26.15	1.59
76201511-3	CFAINT32	P03	120	FCS1 1.53 mW			
82500805-1	5242AS02	P03	180	FCS1 1.42 mW			
82500805-2	5242AS02	P03	180	HR 7310 3×2 nodding	17.67	32.12	1.82
82500805-3	5242AS02	P03	180	FCS1 1.42 mW			
76902105-1	CFREP206	P03	120	FCS1 1.53 mW			
76902105-2	CFREP206	P03	120	HR 6132 3×2 nodding	17.03	27.88	1.64
76902105-3	CFREP206	P03	120	FCS1 1.53 mW			
76902215-1	CFREP206	P03	180	FCS1 1.42 mW			
76902215-2	CFREP206	P03	180	HR 6132 3×2 nodding	17.03	30.57	1.80
76902215-3	CFREP206	P03	180	FCS1 1.42 mW			
76901705-1	CFREP207	P03	52	FCS1 1.42 mW			
76901705-2	CFREP207	P03	52	HR 7854 3×2 nodding	18.84	25.36	1.35
76901705-3	CFREP207	P03	52	FCS1 1.42 mW			
76901815-1	CFREP207	P03	79	FCS1 1.42 mW			
76901815-2	CFREP207	P03	79	HR 7854 3×2 nodding	18.84	29.53	1.57
76901815-3	CFREP207	P03	79	FCS1 1.42 mW			
81900404-1	54205PC	P03	180	FCS1 1.42 mW			
81900404-2	54205PC	P03	180	HR 0794 3×2 nodding	20.37	36.94	1.81
81900404-3	54205PC	P03	180	FCS1 1.42 mW			
81901808-1	54205PC	P03	180	FCS1 1.42 mW			
81901808-2	54205PC	P03	180	HR 0794 3×2 nodding	20.38	36.97	1.81
81901808-3	54205PC	P03	180	FCS1 1.42 mW			
81902312-1	54205PC	P03	180	FCS1 1.42 mW			
81902312-2	54205PC	P03	180	HR 0794 3×2 nodding	20.39	36.46	1.79
81902312-3	54205PC	P03	180	FCS1 1.42 mW			

Table 15: *P3 60 μm absolute photometry of point-sources in non-default apertures. For background measurements the calibrated and colour corrected ISOPHOT and COBE-DIRBE values are given together with the ratio.*

TDT	PROPID	AOT	Aper [″]	Target	$COBE_{cc}$ [MJy/sr]	PHT_{cc} [MJy/sr]	PHT/COBE
44800603-1	524112P3	P99	180	HR 5340 off	8.02	11.66	1.45
44800704-3	524112P3	P99	180	FCS1 1.05 mW			
44800704-4	524112P3	P99	180	HR 5340 on			
44800704-6	524112P3	P99	180	FCS1 0.93 mW			
44801003-1	524113P3	P99	99	HR 5340 off	8.02	11.04	1.38
44801104-3	524113P3	P99	99	FCS1 1.36 mW			
44801104-4	524113P3	P99	99	HR 5340 on			
44801104-6	524113P3	P99	99	FCS1 1.18 mW			
44803006-3	524114P3	P99	99	FCS1 0.83 mW			
44803006-4	524114P3	P99	99	HR 7310 on			
44803107-1	524114P3	P99	99	HR 7310 off	5.14	6.49	1.26
44803208-1	524114P3	P99	99	HR 7310 on			
44803309-1	524114P3	P99	99	HR 7310 off	5.14	6.71	1.31
44803410-2	524114P3	P99	99	FCS1 0.93 mW			
44803501-3	5241M0P3	P99	180	FCS1 0.67 mW			
44803501-4	5241M0P3	P99	180	HR 7310 on			
44803602-1	5241M0P3	P99	180	HR 7310 off	5.14	7.41	1.44
44803703-1	5241M0P3	P99	180	HR 7310 on			
44803804-1	5241M0P3	P99	180	HR 7310 off	5.14	6.78	1.32
44803905-2	5241M0P3	P99	180	FCS1 0.67 mW			
77700405-1	CFREP306	P03	120	FCS1 0.71 mW			
77700405-2	CFREP306	P03	120	HR 0165 3×2 nodding	9.50	10.36	1.09
77700405-3	CFREP306	P03	120	FCS1 0.71 mW			
77700615-1	CFREP306	P03	79	FCS1 0.71 mW			
77700615-2	CFREP306	P03	79	HR 0165 3×2 nodding	9.50	10.55	1.11
77700615-3	CFREP306	P03	79	FCS1 0.71 mW			
77700825-1	CFREP306	P03	180	FCS1 0.71 mW			
77700825-2	CFREP306	P03	180	HR 0165 3×2 nodding	9.51	11.34	1.19
77700825-3	CFREP306	P03	180	FCS1 0.71 mW			
72001502-4	5241AS13	P03	180	FCS1 0.83 mW			
72001502-5	5241AS13	P03	180	HR 7980 3×1 nodding	16.25	19.95	1.23
72001502-6	5241AS13	P03	180	FCS1 0.83 mW			
73401910-2	CFREP305	P03	79	HR 7980 off	18.08	20.63	1.14
73401910-3	CFREP305	P03	79	FCS1 0.71 mW			
73401911-2	CFREP305	P03	79	HR 7980 on			
73401911-3	CFREP305	P03	79	FCS1 0.71 mW			